



Contents lists available at ScienceDirect

Computers & Graphics

journal homepage: www.elsevier.com/locate/cag



Analysis of drawing characteristics for reproducing traditional hand-made stippling

Domingo Martín^a, Germán Arroyo^a, Vicente del Sol^a, Celia Romo^a, Tobias Isenberg^{b,*}

^aUniversity of Granada, Spain

^bInria, France

ARTICLE INFO

Article history:

Received 20 July 2018

Received in final form 13 February 2019

Accepted 13 February 2019

Available online 20 February 2019

Keywords: Non-photorealistic rendering, simulation of natural media and traditional styles, stippling, reproduction based on pixel density

ABSTRACT

We contribute an in-depth analysis of the characteristics of traditional stippling and relate these to common practices in non-photorealistic stippling as well as to the abilities and limitations of existing printing and display technologies. Based on the properties of traditional stipple dots which depend on the used pens and paper types, we focus on a perceptual study of digital stippling that further informs our discussion and work toward an understanding of the requirements for the reproduction of hand-made stippling. To allow artists and illustrators to replicate the stippling process faithfully in the digital domain, we thus extract guidelines from the study results such as that the characteristics of real dots must be reproduced because they are perceived and that the results must be adjusted to the different properties of output devices.

© 2019 Elsevier B.V. All rights reserved.

1. Introduction

Hand-made stippling is an artistic style that represents images using dots. Usually, a pen is used to deposit black ink onto white paper. Although it seems to be an easy technique to master, it requires not only artistic talent but also a lot of training and much time for each individual image due to the need to place many dots. This traditional technique has many advantages: it is economic as it only relies on a single color (good for reproduction), it can represent not only tone but also shape and texture, and dots do not impose an orientation which avoids certain visual artifacts. While stippling is no longer frequently used, it can be found in some scientific domains such as archeology, biology, entomology, etc., as well as in artistic drawing.

Similar to other traditional techniques of artistic expression or illustrative depiction, stippling has also been reproduced in the non-photorealistic rendering (henceforth NPR) domain [1–4]. Computer processing has opened up new possibilities such as the creation frame-coherent animation using a 3D model as input [5] to name just one example. One goal for most stippling

approaches, however, remains the faithful replication of the traditional technique to be applied to new images, e. g., in situations when it is impossible to hire a professional stipple artist.

It can be argued that, while many recent advances including example-based techniques have significantly advanced the quality level of computer-supported techniques, there are still numerous limitations of NPR stippling that remain to be addressed. To be able to make significant advances in the field in the future, we have thus embarked on a study of the traditional technique with the ultimate goal of being able to accurately reproduce traditional hand-made stippling. Our goal is to establish a clear set of conditions and guidelines for an approach to reproduce traditional hand-made stippling. For this purpose we concentrate specifically on the generic problem of reproducing hand-placed stipple dots and the corresponding constraints that arise from the used traditional tools (i. e., paper type, pen sizes, paper-and-pen interaction, resolution-dependence) as well as the goals of digital presentation and reproduction (e. g., display vs. print reproduction, stippling as an art form vs. stippling as a way to fill an area with dots). The results of our study of these low-level aspects of stipple dots can be used in future NPR techniques for faithful NPR stippling. Specifically, we formulate guidelines for

*Corresponding author: e-mail: tobias.isenberg@inria.fr

the replication of stippling as an art form such as the need to include the stipple textures into consideration, depending on the chosen pen/paper combination and output medium.

This article is an extended and edited version of our paper [6] published at Expressive 2015. In particular, in this article we add a detailed perceptual study of stipple dots in Sect. 5 and discuss its implications for digital stipple rendering. We thus contribute:

- A study about the appearance of hand-placed dots in traditional stippling and their physical characteristics. We study dots based on the pens (type, nib sizes) and paper used by different artists to understand what dots result from different materials. Based on this work we establish constraints for the digital reproduction of dot tone, shape, and size.
- A discussion of stipple dot reproduction on typical output devices. When transitioning from traditional hand-made stippling to digital reproduction we face a conversion from a continuous to a digital world. Based on this change we not only discuss the capabilities but also identify several important limitations to consider for digital stippling.
- Based on these considerations and on an experiment that we conducted on how digital stippling is being perceived by human observers if reproduced in print and on a screen, we discuss the effects of the identified dot attributes on the perception of the digitally stippled images and the resulting implications for synthetic stippling. As our take-away message, we provide a list of guidelines for practitioners to decide which aspects of stippling (distribution, resolution-dependence, stipple textures) to focus on, depending on their chosen application domain and form of reproduction.

2. Previous Work in Digital/NPR Stippling

Digital stippling is a technique that was first introduced to computer graphics in the late 1990s. Initially, researchers focused primarily on where to place dots. Most early techniques relied on the concept of Centroidal Voronoi Diagrams (CVD, also called Lloyd’s method [7, 8]): based on an initial dot distribution (e. g., depending on a condition such as tone), the dot distribution’s Voronoi Diagram is computed and the dots are moved to the centroids. This step is repeated until the result is satisfactory.

Deussen et al. [9, 10] were the first to implement this process using an interactive system that used brushes to locally apply Lloyd’s method. Secord [11] generalized this process to use weighted centroidal Voronoi diagrams based on the local tone of the source image. Others such as Hiller et al. [12] and Dalal et al. [13] then extended the general approach to be able to not only place circular dots but general shapes. Researchers have also investigated methods for obtaining a suitable initial point distribution, either to be used in CVD-based stippling or in its own right. Secord et al. [14], e. g., probabilistically distributed primitives in image space—a method that can also be used for frame-coherent animations—, while Arroyo et al. [15] used a Monte Carlo technique sampling an adaptive probability density function. Related to these kind of stochastic methods is also the RenderBots system by Schlechtweg et al. [16] that uses autonomous agents with random processing to place stipples.

Researchers generally investigated ways to avoid the visual problems in point placement that arise from the original version of Lloyd’s method: chain artifacts that stipple illustrators aim to avoid [17]. Balzer et al. [18] presented a capacity-constrained way to create point distributions based on Lloyd’s method that possess blue noise characteristics. Kopf et al. [19] presented a method based on non-repetitive Wang tiles and Poisson disk sampling that also produces point sets with blue noise characteristics and thus both avoids artifacts and facilitates an infinite yet smooth zoom into stipple images. Ascencio-Lopez et al. [20] similarly used Poisson disk sampling but with the goal to produce pleasing distributions at fast speeds. Recently, Deussen et al. [21] introduced weighted Linde-Buzo-Gray stippling as an adaptive version of Lloyd’s method that does not require a good initial point distribution and also converges fast. As an alternative, Deussen [22] generalized Lloyd’s original CVD method using energy-based optimization, e. g., to be able to also produce point clusters instead of only evenly distributed point sets.

While the techniques discussed so far—similar to the artistic example—concentrated on representing 2D still images using stippling, researchers also developed techniques for 3D shape stippling. The transition to 3D models as input not only facilitates forms of expression impossible in traditional stippling (e. g., animation) but also raises the problem of frame-to-frame coherence. To solve it, Meruvia Pastor et al. [5, 23] used a particle system attached to the 3D surface to achieve smooth animation. Lu et al. [24, 25], similarly, placed and tracked surface points and discussed hardware acceleration options. To facilitate the zooming into a model, Meruvia Pastor and Strothotte [26] demonstrated how to use distribution hierarchies with graph-based relaxation. In an approach that aims at simplifying the 3D computation, Yuan et al. [27] derived point distributions for 3D rendering in geometry-image space, achieving frame-to-frame coherence and benefiting from GPU acceleration. Vanderhaeghe et al. [28] went a step further and reverted back to computing point locations in 2D space to optimize their 2D characteristics—yet ensuring that the moving point distribution behaves correctly for 2D projections of animated (rigid or soft-body) 3D shapes. Approaches for other 3D surface models such as point-sampled geometry [29, 30] have also been discussed.

Two special forms of 3D object representations are implicit and volumetric models. For the creation of stippling for implicit, Foster et al. [31] randomly distributed a set of particles onto the model and then used attractor/repulser forces to move the points back to the implicit surface according to its changes as well as with respect to neighboring points. In contrast, Schmidt et al. [32] used a real-time method to extract a low-quality base mesh from the implicit model and then placed surfels [33] on the surface, which in turn carry a hierarchy of stipple dots. In a related approach for Hermite RBF implicit, Vital Brazil et al. [34] densely sampled the implicit surface and then used these seeds to generate stipple dots for the rendering. For volumetric stippling, in contrast, Lu et al. [25, 35] randomly placed stipple points throughout the volume based on the data’s features, out of which the stipple points to be shown at render time were selected based on the viewing conditions.

While these point distributions were largely based on ran-

dom placement, noise qualities, or dedicated distribution processes, researchers recently started to derive the distributions from human input in form of example-based stippling. Barla et al. [36, 37], e. g., synthesized different hatching and stippling styles by extracting the drawing primitives and analyzing their neighborhood relationships. Inspired by earlier analyses of stipple aesthetics [38, 39], Kim et al. [40] followed a similar goal and used a gray-level co-occurrence matrix (GLCM) to capture the statistics of stipple distributions for later synthesis. Martín et al. [41, 42] concentrated on reproducing correct stipple distributions based on pixel density considerations and scanned stipples that can faithfully reproduce the merging of stipple dots.

This last method uses halftoning, which some other stippling methods also employ. For example, Hausner [43] extended error diffusion for generating point distributions for pointillist halftoning. Mould [44] used a progressive distance calculation based on a graph representation of the source image, a method that specifically emphasizes wanted linear features using stipple chains. Li and Mould [45] shared the same goal and proposed a structure-aware stippling approach using an error distribution scheme based on the importance of the different features to be reproduced. A special form of stippling related to such structure-preserving approaches is the reproduction of hedcut images. Here, the stipples are arranged along dedicated lines, related to hatching techniques. Example techniques were presented by Kim et al. [46], Kim et al. [47], and Son et al. [48].

A more comprehensive survey of these and other digital stippling techniques was recently presented by Martín et al. [4] who also provide a taxonomy of the different techniques and discuss their relationship to traditional stippling as well as to halftoning. For more details on the respective methods we thus refer to this survey or to the original literature.

Virtually all these techniques whose goal it is to simulate traditional stippling concentrate on dot placement, either for traditional 2D input or for three-dimensional shapes. The question of how to treat the reproduction of the dots themselves is often not raised, in many cases black circles or pixels are used to represent them. Questions of overlapping/merging dots as well as of whether stippling should be treated as a black-and-white technique are also not frequently discussed, with only few exceptions [40–42]. Even the suitable size of the dots is only rarely discussed. For instance, Deussen et al. [9, 10] vary the dot size based on the image tone, while Secord [11] mentioned size control as future work but implemented tone-based control in his demo tool—albeit only for circular dots. Martín et al. [41, 42], finally, studied examples of scanned dots and based their placement on the physical size of real stipples, computing the needed resolution accordingly. Based on a study of hand-made stippling, we thus extend this general approach and work toward establishing a new framework for digital stippling that aims to faithfully replicate the traditional technique and that focuses on the characteristics of the stipple dots, their physical sizes, the employed paper, and the used output media.

3. From Hand-Made Stippling to Digital Reproduction

Traditional hand-drawn stippling is produced by manually placing dots on paper with a pen, usually with black ink on white

paper. Stipple dots are typically placed intentionally one by one (in no particular order), while trying to avoid visual artifacts [17] unless such artifacts are intended to represent specific features. Stipple dots can overlap each other—very dark zones in an image can be produced using many overlapping stipples.

Like other artistic techniques, stippling comprises three tasks: an artistic, a procedural, and an instrumental task. Only by mastering all three can an artist produce aesthetically pleasing images that convey the intended message, e. g., in an illustration (for a more detailed discussion see our conference paper [6]).

In the *artistic task* the stipple artist selects what to represent and what to leave out, where detail needs to be provided and where a more abstract, simplified representation is sufficient, where to stick to the original source and where artistic freedom can be employed, and other mental processes that are part of the artistic work. These steps have been beyond the scope of NPR support until recently, but recent developments in deep learning and neural style transfer (see, e. g., Gatys et al. [49, 50] and the overview by Semmo et al. [51]) are currently opening up new possibilities that should be explored in the near future.

The *procedural task* refers to the way the ideas and concepts derived in the artistic task are converted into visual artifacts, i. e., the arrangement of dots on the paper. This task, consequently, is the one that most traditional digital stippling techniques have supported by deriving stipple dot distributions based on some input data. Beyond a personal style, the procedural task also refers to stylistic choices such as the regularity of the dot placement, the density of the dot placement, and the use of effects such as overlapping. These different strategies can be used, e. g., to replicate different materials and textures of the depicted objects.

The *instrumental task*, finally, refers to the media and tools that are used in the stippling process and the low-level actions for placing the dots with the chosen tool onto the chosen medium. Here it is important to mention that the human visual system works at different levels of details simultaneously, ranging from the small part of the focus of attention to aspects of an image that are perceived about the rest [52].

As the artistic task is beyond the current abilities of NPR techniques and because the procedural task is relatively well supported in our field already, we decided to focus on the instrumental task. Ultimately, our goal is to support stipple artists in the two lower-level tasks for computer-supported stippling, allowing them to concentrate on the artistic choices (like others have done for other traditional artistic media such as pencils [53–55], watercolor [56], oil paint [57, 58], and wax crayons [59]). We thus focus in the physical characteristics of physically placed dots, their shape, their size, their tone, as well as the possible relations between these characteristics. Similar to the lower-level characteristics of dot distributions, these attributes can have a significant influence on the final result, which motivates us in studying them to provide a solid foundation for a wide variety of existing and future digital stipple techniques.

To establish this foundation we need to understand to what degree a digital stipple dot can resemble a hand-made stipple dot, based on the type of digital reproduction. Therefore, to be able to transition/transfer from the continuous physical domain to the discrete digital domain, we need to understand both the

Table 1. Tool/material preferences of the collaborating professional artists.

Illustrator	Pen type	Nib size	Paper type
Randy Glass	Rotring Rapidograph	0.13mm	FLAX (Medium press)
Miguel Endara	Sakura Pigma Micron Pen 005	0.20mm	Strathmore 500 Illustration Board (Hot press)
Elena Piñar	Artline Drawing System	0.50mm	Canson Watercolor (Cold press)

characteristics of traditionally hand-made dots as well as the constraints of the digital reproduction such as pixel density, color resolution, and reproduction medium (printing on paper vs. display on the screen) as all these aspects influence the final perception of the result. To thus obtain a solid basis for this study of realistic hand-placed stipple dots, we started by contacting two professional illustrators, Miguel Endara and Randy Glass, as well as a part-time illustrator, Elena Piñar.¹ Specifically, we asked them about their use of paper and pen types for their stipple work (a summary of these preferences is shown in Table 1).

Based on this information we set out to create a dataset to allow us to compare the different pen and paper types. We decided focus on these aspects and leave out pressure and pen angle—the pen is held upright and we kept pressure constant as we expected it to affect the outcome proportionally for different paper and pen types. We asked a skilled fine arts student² (fourth year, for whom stippling is part of her education) to draw 5 different tones out of a gray ramp, using the three different pens from Table 1 and three different types of paper. The latter choice of paper is equally important as the pen type as, for example, cold press paper has texture, absorbs the ink quickly, and spreads it, while hot press paper is smooth, absorbs the ink more slowly, and does not spread it. We thus used a cold press paper (Canson Watercolor; 370g/m²), a medium press paper (Canson Graphics Art; 224g/m²), and a hot press paper (Canson Technical Drawing; 160g/m²).

We then digitized the resulting samples using an Epson Perfection V700 Photo scanner with an optical 4800 ppi pixel density.³ Fig. 1 shows example sections from these scans, each a 1200 × 1200 pixel part from the scan (more examples are shown in the conference paper [6] and the additional material). They clearly show that stipple dots vary significantly in size and shape. Expectedly, the size depends primarily on the size of the pen’s nib, yet also varies for dots created with the same pen on the same paper. We also see that both the size and the dot boundaries depend on the paper type, with cold press paper leading to more ink absorption artifacts than medium and cold press paper. This diffusion/absorption can be seen, in particular, in Fig. 2(c)—the effect being stronger for pens with larger nib sizes.

To look at the individual dots even more closely we also show 240 × 240 pixel detail sections at a 40× magnification in Fig. 2 (more examples in the conference paper [6]). For comparison, we included circles with diameters of 25 pixels, 38 pixels, and 94 pixels, respectively, corresponding to the sizes of the nibs of

0.13 mm, 0.2 mm, and 0.5 mm at 4800 ppi. In the figure we can observe that the overall sizes of the actual stipples deviate from that of the pen’s nib; in our case they are larger for the small and medium nib sizes and smaller for large nib size (it depends on the chosen pens as well as used pen orientation and pressure). We can also clearly see, in particular in Fig. 2(c), that the dots are never completely black. Instead, they exhibit a pattern of gray shades that depends on the used paper, as previously pointed out [41, 42]. This is, in fact, to be expected as the paper-ink interaction is similar to that of watercolor (e. g., [56, 60]).

4. Dot Reproduction: Potential & Limitations

The results of digital stippling can be displayed on a variety of output media, the main types being presentation on a screen and print reproduction. These forms of reproduction, however, have quite different capabilities and limitations. The same result such as in the form of a PDF document can even be intended to both being shown on the screen and being printed. We thus discuss the different capabilities and limitation next.

4.1. Printing

Let us first focus on printing because, in that case, the result is reproduced on paper, similar to the hand-made original. While several traditional printing techniques exist, in today’s digital world we typically use either laser printers or inkjet printers. Both place toner or ink dots on paper, either just in black or using CMYK primaries. All these technologies, however, share the same limitation that they can only use pure colors/toner/ink and are not able to directly produce shades of gray or of a color. This means that the result of any stippling technique that uses scanned or simulated grayscale stipple dots needs to undergo a conversion to a binary dot pattern that resembles the intended gray values. This conversion, of course, is subject to the printer’s output pixel density as we showcase next.

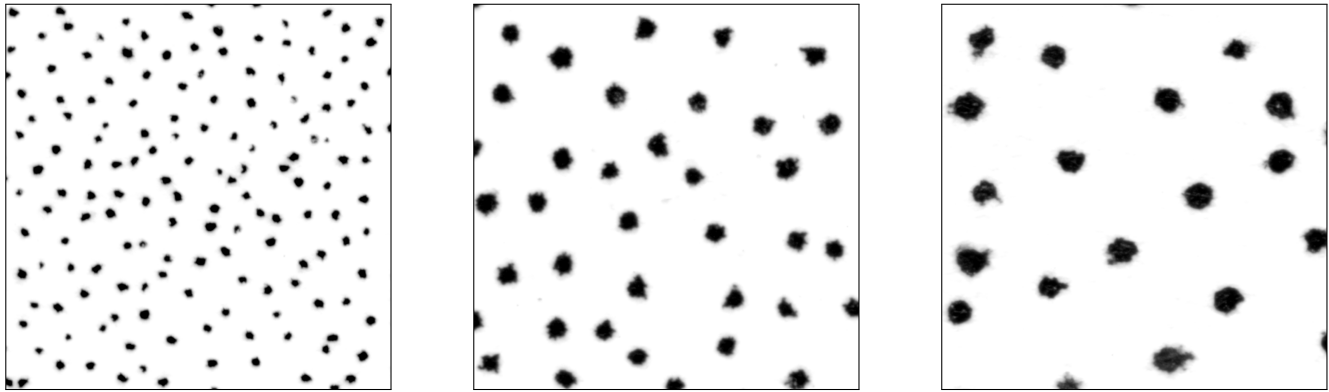
For our discussion we assume that we are interested in reproducing the stipple image with a realistic spatial size (like also done by Martín et al. [41, 42])—similar in dimension to hand-made originals such that the stipple dots have the correct size. Based on this assumption and the measurements discussed in Sect. 3 we can analyze the effects of the printing process. Table 2 lists the number of horizontal or vertical dots that are available to represent a single stipple, depending on the printer’s pixel density and the used nib sizes. We can see that, for a 0.13 mm pen and a 300 dpi printer, less than 2 × 2 printer dots are available to completely represent the stipple. This is not only not enough to show a circle, it is also certainly not sufficient to represent the complex shapes and texture of real stipples.

For today’s printers, which typically operate at 1200 dpi, the situation appears to be better: we have 6 × 6, 9 × 9, and 24 × 24 dots available for stipple sizes of 0.13 mm, 0.2 mm, and 0.5 mm, respectively. This may seem to be sufficient to capture the stipple shape, at least for the larger pen sizes. We have to take into account, however, that to be able to also represent the stipples’ textures the printer has to use some form of halftoning [61]. Halftoning trades spatial pixel density for tone (color) resolution, so this process reduces the effective pixel density that is available

¹See their work at <http://miguelendara.com/> and <http://www.randyglasstudio.com/> as well as in Fig. 1 of our conference paper [6].

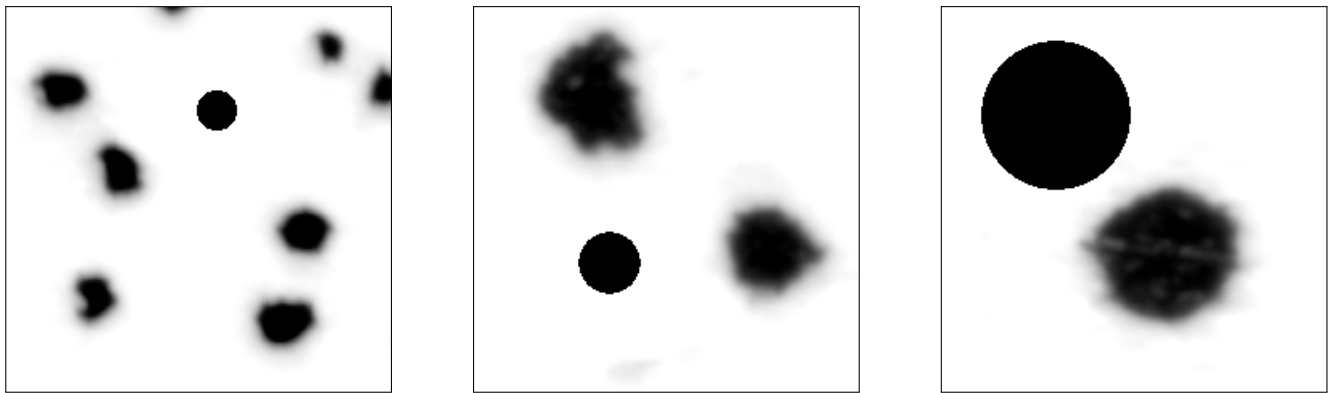
²To study the low-level aspects of instrumental task it is not necessary to rely on the artistic skills of a professional stipple artist.

³We distinguish between ppi as a unit when we discuss pixels in scanning and image processing and dpi when we talk about the dots in the printing process.



(a) Rotring rapidograph 0.13, 0.13 mm, cold press paper. (b) Sakura Pigma 005, 0.20 mm, medium press paper. (c) Artline 0.5, 0.50 mm, hot press paper.

Fig. 1. Three samples from the stipple dot experiments shown at 8× magnification.



(a) Rotring rapidograph 0.13, 0.13 mm, cold press paper. (b) Sakura Pigma 005, 0.20 mm, medium press paper. (c) Artline 0.5, 0.50 mm, hot press paper.

Fig. 2. Details from Fig. 1 at 40× magnification, with black circles added that represent the nib sizes of the used pens.

to represent stipples by at least 3 in each direction, thus to a maximum of 2×2 , 3×3 , and 8×8 , respectively—in most cases not enough for an adequate reproduction of the stipple shapes. For a proper representation of 256 gray levels it would even be necessary to reduce the spatial pixel density by 16 in both directions using AM halftoning [61–63] or by a factor of 8–12 using error diffusion [64]. Moreover, the halftoning process introduces dot patterns that are supposed to emulate gray values. These patterns can still be perceived by humans at 1200 dpi when looked at from a typical reading distance of 25 cm–60 cm [63] and thus interfere with the perception of the stipple dot pattern.

The reason for this effect is the *visual acuity* of the human visual system [63, 65]. Visual acuity is based on the limit of feature recognition for humans of 1 arc minute. For example, as Table 3 shows, at a reading distance of 50 cm people can distinguish features of approx. 0.14 mm, corresponding to 183 dpi (or ppi). While this result would suggest that a 1200 dpi printer is sufficient for reproducing the gray values using halftoning, we have to take the size of the halftoning patterns into account that create the illusion of tone shades and multiply the needed pixel density by this size as demonstrated in the two last rows of Table 3. This means that, for typical reading distances, at least a 2400 dpi printer is necessary such that the dot patterns from halftoning are no longer perceived [63]. Another limitation of, in particular, laser-based printing can have an influence on how printed stippling is being perceived by observers: the “dot gain”

effect is “the increase in size of a printed dot from its intended size” [66]. Lau et al. [66] describe how dot gain can result in isolated white pixels being filled by surrounding black regions, and that it can also lead to patterns that are darker than intended with the original black-to-dark ink ratio.

4.2. Display on a Screen

A different situation arises when we try to display stipple images on screens. Regardless of whether they use CRTs, LCDs, or OLEDs as their underlying technology, screens have the important benefit of being able to show color gradients—typically with at least 8 bits per color, newer devices with up to 12 bits per color. The same is true for e-ink displays, although the current technologies are limited to 4 bits or 16 shades of gray. They all are thus well able to depict the tonal aspects of stipple dots.

A problem arises due to the limited spatial density of today’s screens as illustrated in Table 4. Current devices use spatial densities of approx. 100 ppi, even newer UHD displays have ≤ 200 ppi. Also the most recent e-ink displays have a maximum density of 300 ppi. Only some mobile phones have reached pixel densities of more than 300 ppi, but their physical screen space is too small to be considered for the display of stipple images.

Using 112 ppi as an example for a typical screen pixel density, each pixel has the size of $0.23 \text{ mm} \times 0.23 \text{ mm}$. It is thus not possible to use more than a single pixel to represent a stipple dot when showing stipple images at their correct size—less than

Table 2. Number of printer dots available to represent a stipple dot, depending on print dot density and pen’s nib size.

Nib	300 dpi	1200 dpi	2400 dpi	4800 dpi
0.13mm	1.54	6.14	12.28	24.57
0.20mm	2.36	9.45	18.90	37.38
0.50mm	5.91	23.62	47.24	94.49

Table 3. Maximum perceivable dot/pixel density depending on the viewing distance for 100% visual acuity. Resulting need for dot density in dpi when halftoning is used.

	25 cm	35 cm	50 cm	100 cm
mm per dot / pixel	0.07	0.10	0.14	0.28
dpi / ppi	366	261	183	91
needed dpi w/ halftoning, 8×	2926	2090	1463	732
needed dpi w/ halftoning, 16×	5852	4180	2926	1463

Table 4. Pixel densities in ppi for common monitor sizes and pixel counts. The most commonly used types in bold.

Size	1360 × 768	1920 × 1080	2560 × 1600	3840 × 2160
15"	104	147	201	294
24"	65	92	126	184
27"	58	82	112	163
30"	52	73	101	147
32"	49	69	94	138

Table 5. Number of (horizontal/vertical) pixels available to represent a single stipple dot, based on the pen’s nib size.

Nib	76 ppi	92 ppi	112 ppi	138 ppi
0.13 mm	0.4	0.5	0.6	0.7
0.20 mm	0.6	0.7	0.9	1.1
0.50 mm	1.5	1.8	2.2	2.7

one pixel is available to show stipples for pens with nib sizes of 0.13 mm and 0.2 mm. Table 5 shows a summary of the number of pixels available for a single stipple dot, depending on the pen’s nib sizes and the display’s pixel density. Most displays have less than 2×2 pixels to show a single stipple, and even the most high-resolution ones provide less than 3×3 pixels. This means that, while screens would be able to show the grayscale properties well, they do not have a sufficient pixel density to represent the irregular shapes of realistic stipple dots.

5. Analysis of Stipple Dot Perception

Beyond this discussion of the real dot’s characteristics based on magnified scans and the two major possibilities of reproduction of scanned or digitally produced stippling, we also wanted to understand how stipple dots are perceived by humans under changing conditions—in particular to understand if it makes a difference whether we invest effort into faithfully synthesizing real stipple dots or using scanned exemplars, as opposed to simple black circles. For this purpose we carried out two experiments, a first small one (pilot survey) and, based on its results, later a more detailed study. We describe both experiments next.

5.1. Pilot Survey

To get a first indication on people’s perception of stipple dots we recruited 11 unpaid volunteers (7 females; ages in the range of 22–25; fine arts graduate students from the local university population). All had experience in drawing with pen and ink,

including stippling. We asked them to examine the previously created (Sect. 3) original, hand-made paper samples and to evaluate them based on their tone (black vs. gray), shape (round vs. irregular), and size (constant vs. varying). For this purpose the participants were seated on a desk which was lit with a constant, artificial fluorescent light source, and participants went through the stack of images in randomized order, filling out a questionnaire as they progressed.

Table 6 shows the results of this small perceptual survey. The data suggests that, in many cases, the stipple dots are indeed perceived as being black, but for some combinations of nib size and paper a considerable number of people perceives them as being rather gray—smaller dots more often seem to be perceived as being gray. It is interesting to note that, despite the discussed differences in diffusion/absorption for cold press paper vs. medium and hot press paper, our participants perceived the 0.5 mm pen on cold press paper as black, while 27% of our participants saw the dots of the same pen on hot press paper as gray. Also, a large number of participants did perceive the irregularities in shape and size as we expected.

5.2. Detailed Analysis of Stipple Dot Perception

Based on these initial results we then set out to conduct a more detailed and elaborate perceptual experiment. While the theoretical discussions in Sect. 4 inform us about the potential limits of the perception of stippling and stipple dot properties, but to get to practical design guidelines for how to represent and reproduce stipple dots we also need empirical study results. Our personal experiences with traditional computer-generated stippling showed us that the completely black and partially circular stipples of the past were accepted by the community, while our observations of physical hand-made stippling results suggested that, depending on nib size and paper type, some dots may indeed be perceived as black dots on white background.

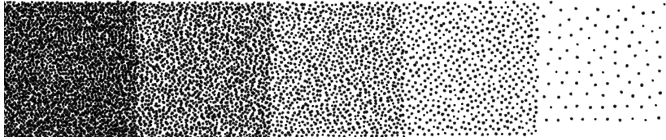
Specifically, we thus wanted to investigate the *practical* implications of using black-and-white laser printers as well as RGB screens as output devices (based on our discussion of their potential and limitations in Sect. 4), with respect to how they are perceived by human observers. Essentially, we wanted to see if the characteristics that can be found in physical hand-made stipple samples are perceived by human observers when looking at them in the form of digital reproductions or simulations.

5.2.1. Physical Study Setup

Generally, we based our study setup on the generation of various dot samples for which their tone, shape, and size characteristics are varied in a controlled way. To allow participants to then realistically compare screen-displayed and printed stippling using these samples, we have to take the considerations in Sect. 4 into account and setup our study environment accordingly. We used 300 mm as the distance at which we want to ask our participants to observe the samples—a typical reading distance. According to the considerations on visual acuity in Sect. 4.1, the corresponding 1 arc minute limit for recognizable features results in a minimum pixel density of 291 ppi. We thus used a slightly higher value of 300 ppi as our target density—consistent with the pixel density used, for the same reason, in commercial printing.

Table 6. Results of the perceptual survey for tone, shape and size; depending on the paper type and the pen’s nib sizes (in mm). The numbers indicate the percentage of people who answered in the respective fashion.

feature	cold press paper			medium press paper			hot press paper		
	0.13	0.2	0.5	0.13	0.2	0.5	0.13	0.2	0.5
tone (black / gray)	73% / 27%	82% / 18%	100% / 0%	100% / 0%	91% / 9%	100% / 0%	55% / 45%	55% / 45%	82% / 18%
shape (regular / irregular)	55% / 45%	36% / 64%	27% / 73%	36% / 64%	45% / 55%	45% / 55%	64% / 36%	9% / 91%	0% / 100%
size (constant / varying)	91% / 9%	36% / 64%	27% / 73%	55% / 45%	45% / 55%	55% / 45%	64% / 36%	27% / 73%	9% / 91%

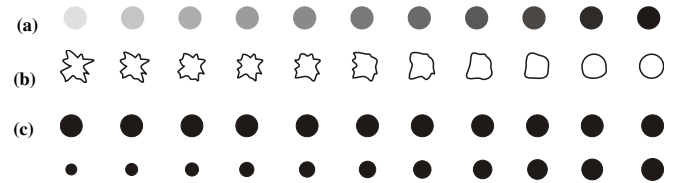
**Fig. 3. Example of a five-step ramp used in the test, based on actual stipple dot scans. Each tone field was of size 1 in × 1 in (25.4 mm × 25.4 mm).**

Print setup. For a target pixel density of 300 ppi, 1200 dpi laser printers are usually not sufficient to produce 256 or more tone levels as discussed in Sect. 4.1 and shown in Table 3. AM or clustered halftoning, however, can emulate 17 gray tones for a 300 ppi source image [62], error diffusion methods (e. g., [67, 68]) can even increase this number to 25–34 tones for the same 300 ppi input [64]. This number of tones is higher than the 16 tones used in current e-paper displays, it is sufficient to produce reasonably rich tonal changes, and we thus used an error diffusion process to produce and print the images for our study.

Display setup. As outlined in Sect. 4.2, typical computer displays and TV screens do not reach pixel densities as needed for showing stipple images of A5–A4 size at 300 ppi. We can, however, achieve a comparable effect by using a lower-density display placed at a higher observation distance. For example, a 15.6 inch display with 1920 × 1080 resolution (i. e., 141.2 ppi), each pixel has a size of 0.1799 mm × 0.1799 mm. To make this comparable to a virtual 300 ppi pixel at reading distance of size 0.0873 mm × 0.0873 mm, the physical display has to be placed at a distance of approx. 650 mm from the viewer. The 15.6 inch display can then, however, only display (virtual) images of a maximum size of approx. 160 mm × 90 mm—roughly A6 size.

5.2.2. Study Materials and Trials

As noted above, we were generally interested in understanding if the differences of stipple dot size, texture, and shape that we had observed in our dataset (Sect. 3) can be portrayed by the two main types of output media and whether such variations can be perceived by human observers. For that purpose we used our previously published example-based grayscale stippling technique [41, 42] to produce, like in our hand-made examples from Sect. 3 and using stipple dot scans from these examples, a five-step ramp for each combination of nib size and paper type (e. g., Fig. 3). Our example-based technique is based on real dots, preserves the tone distribution of the stipple dots, can reproduce them correctly at a target size with a target pixel density, and implements the diffusion process by allowing the blending of tones. We thus did not manipulate the stipple dot scans that we used as input other than to apply a linear tone remapping such that the background was pure white (255), while the value

**Fig. 4. Abstract property ramps used in the isolated single-tone test: (a) dot tone, (b) dot shape, and (c) dot size range (for each step in (c), the top and bottom dots indicate the size range).**

of the darkest tone remained unchanged (typically a change of less than 2%). We then used our approach to arrange the dots, adjusted to the needed output pixel densities for the screen and paper conditions. We thus had 9 different ramps (3 nib sizes and 3 paper types). For producing the interpolated and extrapolated versions of the dots, we created a new diffusion-based method (see Appendix A).

Isolated single-tone test (first part). For each ramp and inspired by our preliminary survey, we selected the light-most field (i. e., 9 versions of the sparsest dot distribution, based on the 3 × 3 nib size/paper type combinations) and asked our participants to compare the dots against abstract eleven-step scales of the dot characteristics *tone*, *shape*, and *size range* shown in Fig. 4(a)–(c), respectively. The tone ramp (Fig. 4(a)) was designed to range from 10% gray to full black, the shape ramp (Fig. 4(b)) was designed to range from a (subjectively chosen) dot with a clear non-circular shape to a complete circle, and the abstract size range ramp (Fig. 4(c)) was designed to range from two circles where one has twice the diameter of the other to two equi-sized circles. In total, we thus ended up with 3 nib sizes × 3 paper types × 3 dot characteristics × 2 conditions = 54 trials for this first part of the experiment. With these comparisons we wanted to understand our participants’ perceptions of the characteristics of the individual dots, not of the field as a whole. In contrast to the pilot survey described in Sect. 5.1, we expected to see the distributions of dot characteristic perceptions, as opposed to the previous forced binary choices. This first part, however, is limited in that it will not tell us, for example, what tone level participants actually perceive.

Clustered five-tone test (second part). In a second part of the experiment we thus asked the participants to compare each of the previously described ramps that were generated using scanned dots with similar ramps for which we changed the dot attributes. This time we asked the participants to consider the entire ramp for the comparison to better represent a realistic application case but without having to select any particular example image. We thus created ramp alternatives by adjusting the dots’ sizes, shapes, and tone to understand how well participants perceive changes from the observed (scanned) real dots.

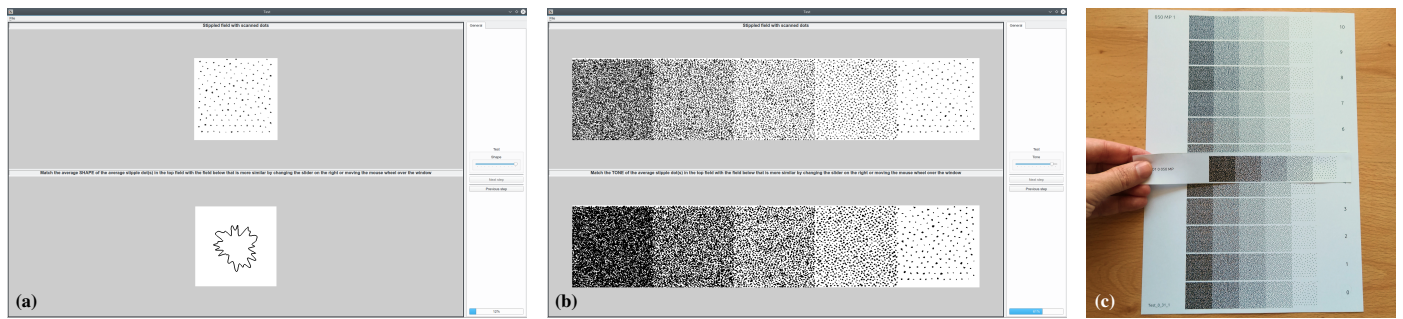


Fig. 5. Study setup: screenshots of the display-based comparison, (a) first and (b) second study parts; (c) paper-based comparison, second study part.

For the dots' **tone** values we first determined the possible extremes of a possible adjustment. Starting from the real scans the dark-most extreme seems obvious: all non-background pixels of a dot are turned into completely black pixels. For the light extreme we selected a contrast and brightness filtering based on human input: In a pilot, we provided 22 colleagues of ours with a tool that showed them the same dot distribution once in its dark extreme, once using the real dots, and once in a light extreme that they could adjust. We then asked them to adjust brightness and contrast of this light extreme such that the respective image completes the tonal range as they would “imagine it.” We used the mean brightness and contrast offset of the results to produce the light-most extreme version of the scans. Based on both extremes and the real scan as the center level, we then used linear interpolation to create eight additional tone levels.

For the **shape** our goal was, inspired by the distinction between round and irregular dots used in our pilot (Sect. 5.1), to understand how people perceive a range of different dot shapes. While the realistic choice (scanned dot) and the round extreme (filled circle) are clear, we also wanted extend the range of shapes toward a more extreme irregular shape that is, nevertheless, inspired by the real dot. This way we ensure that the realistic choice, like for the previously described factor tone and the factor size described next, is in the center of the range of presented choices. To thus create interpolation samples of the transition between a scan and a circular dot we used an interpolation scheme, while we extrapolated from a scan toward a more extreme version using another process. Both novel techniques are described below in Appendix A.

Finally, for the **size**, we increased and decreased the sizes of the scanned points by up to 50% using linear interpolation of the original high-resolution textures, so the ramp with the largest dot uses a factor of 1.5 for the horizontal and vertical dimensions, while the ramp with the smallest dots used a factor of 0.5.

For each of these three characteristics, we thus created 10 additional versions beyond the real scans so that, together with these original dots, we had samples for a 11-point Likert scale [69] choice, from which we asked our participants to select the one that most closely matched the separate sample that we had created based on the original scanned dots. Because we asked our participants to compare the samples with our synthetic stippling proposals according to the same characteristics (nib size, paper type, dot characteristics, and paper/display condition) we again had an experiment with 54 trials per participant.

For the print-based parts of the experiment, we thus gave the participants one printed sheet with the sparse dot fields to compare with (first part) and one printed sheet with the 11 ramp alternatives for each condition (second part), with the ramp to match in the second part being an individual strip of paper they could move next to any of the ramp alternatives (Fig. 5(c)). For the display-based part, we showed the dot fields (Fig. 5(a)) or ramps (Fig. 5(b)) on-screen, with the second part always only showing a single ramp alternative (through which the participants could cycle with button presses or with mouse wheel actions) as well as the ramp we asked them to match (Fig. 5(b)).

5.2.3. Participants and Procedure

For our experiment we recruited 36 unpaid participants (24 female, 12 male), all students of fine art, aged 19–70 years (median: 21.5 years, mean: 23.8 years, standard deviation: 9.98 years). Out of all participants, 3 stated that they have never seen stippling before, while 14 said they had seen it a few times before in their lives, 7 said that they look at stippling images 1–3 × per year, 11 said that they look at stippling images 1–3 × per month, and one stated to look at them 1–3 × per week. While 13 of all participants answered that they had never created stipple art before, 17 participants answered that they created stippling a few times in their lives, and 6 said that they create stipple art 1–3 × per month. All participants had normal or corrected-to-normal vision, with 20 using glasses or contact lenses.

We carried out the experiment always using artificial lighting, a fluorescent light source with a 4000 K color temperature. To maintain the target distance between the eyes of the participants to the stimuli, we instructed them to use the long side of an A4 page (length: 297 mm) as a guideline (1 × for images, 2 × for the screen). For the display-based study part we used 23” screens with 1920 × 1080 resolution, adjusted to our illumination setting and positioned according to our considerations above.

We always grouped the trials by presentation style (paper-based vs. display-based), the order of which we counter-balanced. Within each group, we also counter-balanced the order of samples (i. e., combinations of 3 paper types and 3 nib sizes) using two balanced Latin Squares (due to the odd number of combinations), so that we ended up with $2 \times 2 \times 3 \times 3 = 36$ different trial sequences, one for each participant. For each of the trials, participants first answered the isolated single-tone test questions, followed by the matching questions with the 11 sample ramps (clustered five-tone test). We used ordered sequences for the single-tone tests (with randomly selected default

Table 7. Hypotheses for the first part of the study, for individual dot (a) tone, (b) shape, and (c) size perception, for printer/display reproduction. Each table provides our hypothesis w.r.t. the three different nib sizes and the three different paper types (Cold Press, Medium Press, and Hot Press).

(a) Tone (BW only, GRAY tones).				(b) Shape (IRRegular, CIRcular).				(c) Size range (DIFferent, EQUal).							
0.13		0.20		0.13		0.20		0.13		0.20		0.50			
CP	BW/BW	BW/BW	BW/GRAY	CP	IRR/IRR	IRR/IRR	IRR/IRR	CP	EQU/EQU	DIF/DIF	DIF/DIF	CP	EQU/EQU	DIF/DIF	DIF/DIF
MP	BW/BW	BW/BW	BW/GRAY	MP	IRR/CIR	IRR/CIR	IRR/IRR	MP	EQU/EQU	DIF/DIF	DIF/DIF	MP	EQU/EQU	DIF/DIF	DIF/DIF
HP	BW/BW	BW/BW	BW/GRAY	HP	IRR/CIR	IRR/CIR	IRR/IRR	HP	EQU/EQU	DIF/DIF	DIF/DIF	HP	EQU/EQU	DIF/DIF	DIF/DIF

Table 8. Hypotheses for the second study part, for our participants' ability to find the correct stipple ramp synthesis result based on the dot (a) tone, (b) shape, and (c) size ranges we synthesized for printer/display reproduction. Each table provides our hypothesis w.r.t. the three different nib sizes and the three different paper types (Cold Press, Medium Press, and Hot Press), marked as LOW, MEDium, or LARge standard deviation.

(a) Tone.				(b) Shape.				(c) Size range.							
0.13		0.20		0.13		0.20		0.13		0.20		0.50			
CP	LAR/LAR	LAR/MED	LOW/LOW	CP	LAR/LAR	LAR/MED	LOW/LOW	CP	LAR/LAR	LAR/MED	LOW/LOW	CP	LAR/LAR	LAR/MED	LOW/LOW
MP	LAR/LAR	LAR/MED	LOW/LOW	MP	LAR/LAR	LAR/MED	LOW/LOW	MP	LAR/LAR	LAR/MED	LOW/LOW	MP	LAR/LAR	LAR/MED	LOW/LOW
HP	LAR/LAR	LAR/MED	LOW/LOW	HP	LAR/LAR	LAR/MED	LOW/LOW	HP	LAR/LAR	LAR/MED	LOW/LOW	HP	LAR/LAR	LAR/MED	LOW/LOW

selections in the display condition), and for the five-tone tests randomized the sequence of the ramps differently for each condition, and differently for each participant. The questions about size, tone, and shape, however, always followed the same sequence. Overall, each participant thus completed 2 (display vs. paper) \times 9 (nib size/paper type combinations) \times 3 (tone, shape, size) \times 2 (isolated single-tone vs. clustered five-tone test) = 108 trials, for a total of 3888 trials due to our 36 participants.

For each experiment, two experimenters greeted the participants, described the study, and collected demographic data and informed consent. If the participants had questions during the study, they could ask them any time and the instructors answered them. In addition, the instructors oversaw the data collection to ensure that all questions were answered. Each study session took approximately 46–60 minutes per participant (20–40 minutes for the paper-based part and 15–20 minutes for the screen-based part). We split the experiment into two sessions, 18 participants did the paper condition in one day and the display condition the next day, the other 18 participants did it the other way around.

5.2.4. Hypotheses

As indicated by the three different dot properties we included in the study, we hypothesized that there will be differences in perception of them depending on the nib size, paper type, and way of reproduction. With respect to tone, we hypothesize (**H1**, Table 7(a)) that 0.13 and 0.20 dots will be seen as black only due to their small size, the 0.50 dots could potentially be seen as dots with a different tone. However, for print reproduction (**H1(a)**) even the 0.50 dots will be seen as black dots due to the limited number of tones that are available from the halftoning process. Only for dots shown on a display (**H1(b)**) the 0.50 dots will be seen as having a texture with non-black tones. This hypothesis contrasts the observations from our pilot study (Table 6), yet we believe that the limitations of both computer screen and print reproduction which prevent the textures to be perceived for small dots will have a stronger effect than the influence of the small size on the overall tone perception of the dots.

Second, we hypothesize (**H2**, Table 7(b)) that, due to the small size of the edge 'features' for the smaller dots, 0.13 and 0.20

dots will generally be perceived as circular, only the 0.50 dots will be perceived as irregular. However, due to the higher spatial pixel density of the print reproduction, those dots will be seen as irregular shapes for all sizes (**H2(a)**). In addition, cold press paper leads to larger dot sizes such that participants will also perceive the irregularity of dots shown on the display for all tip sizes, but will be perceived as circles for 0.13 and 0.20 dots with medium and hot press, while the larger size of 0.50 dots allow to be seen as irregular in all cases (**H2(b)**).

Third, we hypothesize (**H3**, Table 7(c))—largely in line with the pilot tests (Table 6)—that the size for the smallest dots (nib size 0.13) will be perceived as more or less constant, while the sizes of larger dots will exhibit a perceivable size range. This applies to all paper types and both types of reproduction/display.

We have thus expressed our hypotheses for the isolated single-tone test as extremes, despite using Likert scales in the experiment. We do this on purpose because we do not have enough data for a more fine-grained prediction. The actual data will allow us to analyze whether the data is indeed centered around the extremes or if the perceptions spread further across the spectrum.

For the clustered five-tone test we formulate hypotheses similar to those of the first part of the study. Based on our previous observations with real stipple images, we hypothesize (**H4**, Table 8) that our participants are better able to match the target gray ramp with the correct synthesis result based on the larger number of information they have—with the possible exception of dot tone for the 0.13 nib size because in this case only little variation is visible. We thus formulate our specific hypotheses by means of the size of the expected standard deviation around the mean of the observations (see Tables 8(a)–(c)).

5.2.5. Results

We analyzed our Likert scale ratings of our experiment using estimation techniques using simple effect sizes and confidence intervals (CI) based on the bootstrapping approach [70].⁴ This procedure follows APA recommendations [71] and addresses the

⁴See the additional material for the anonymized raw data and more summary results in tabular form.

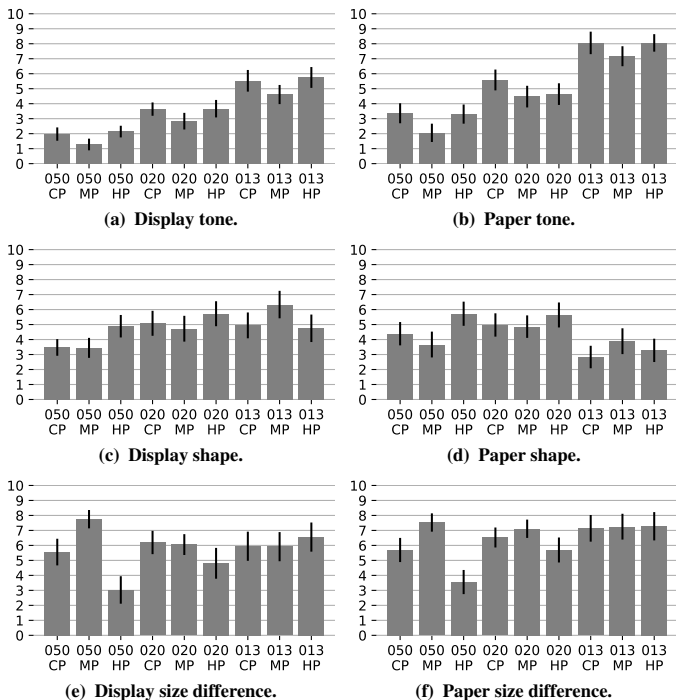


Fig. 6. Means of isolated single-tone tests for the different media/parameters; error bars show bootstrapped 95% confidence intervals (CIs). For (a), (b) tone, 0 is 100% black and 10 is 10% gray. For (c), (d) shape, 0 is a circle and 10 is the most irregular shape. For (e), (f) size difference, 0 is the biggest difference (half diameter)

recent critique of Null Hypothesis Significance Testing (NHST) within statistics and application domains [72–74]. We refer readers who prefer NHST-based statistics to the guidelines by Krzywinski and Altman [75] to infer p -values from our results.

Fig. 6 shows the result of this analysis for the isolated single-tone test, for the display and paper conditions, for all three tested dot characteristics. The graphs show the means from all 36 participants as well as the 95% confidence intervals. Fig. 7 shows the respective graphs for the clustered five-tone test. To better be able to understand the differences between the display and paper conditions, we also computed pair-wise differences for all conditions. We show these differences in Fig. 8, both for the isolated single-tone test and the clustered five-tone test.

5.2.6. Discussion

Next, we discuss the individual results, including differences between display and paper conditions.

Isolated single-tone tests. As one can see in Fig. 6(a) and (b), the *tone* perception for both the screen and the paper condition changes with the dots’ size, with large dots being perceived as almost black (85–95% black), while small dots being perceived as grayish (45–55% black). Yet even the largest dots (left) are not perceived as completely black, so that grayscale-based stippling techniques [41, 42] are needed for a faithful reproduction. The fact that smaller dots are perceived as gray when printed relates to the reproduction technique of halftoning [61]—they are perceived as groups and merge with the background. The correlation values in Fig. 8(a) show us that the dots are perceived quite similar between display and paper, yet overall with a lighter gray values in the paper condition than in the display condition.

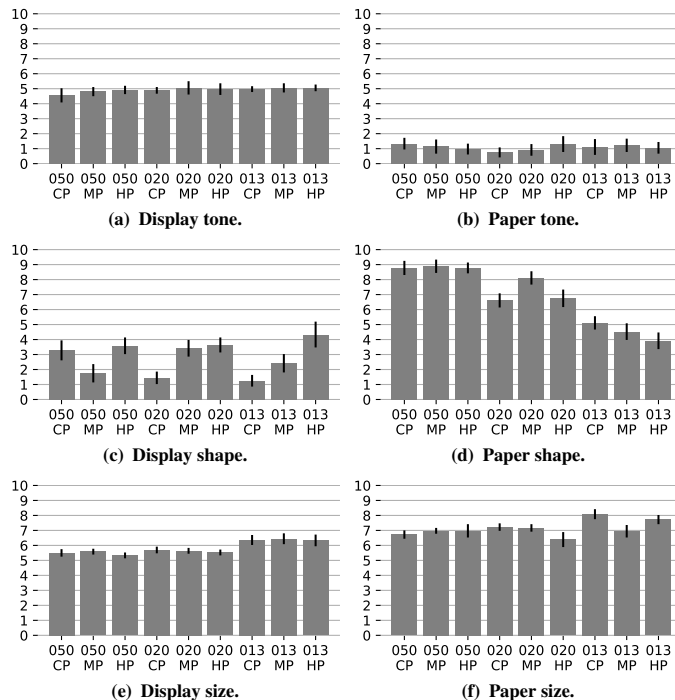


Fig. 7. Means of clustered five-tone tests for the different media/parameters; error bars: 95% CIs. For (a), (b) tone, 0 is 100% black, 5 is the original tone, and 10 is our light extreme. For (c), (d) shape, 0 is a circle, 5 is an original shape, and 10 is the most irregular shape. For (e), (f) size, 0 is $0.5 \times$ the original size, 5 is the original size, and 10 is $1.5 \times$ the original size.

Next, our results (Fig. 6(c),(d)) show that our participants perceived the dots’ *shape* as irregular. Interestingly, small dots (right) for CP and MP paper were seen as more irregular than large ones (left) for the screen condition. We assume that this effect is due to the fact that they are represented with few pixels (e. g., a round dot can hardly be represented with 3 pixels). For the paper condition, in contrast, small dots for CP and HP paper were seen as more round than those created for larger pen tips, probably due to dot gain (see Sect. 4.1 and the work by Lau et al. [66]). Between the paper and display condition, differences only arose for the 0.13 pen tip (Fig. 8(c)). Overall, we conclude that stipples are not perceived as circles, but as irregular shapes.

Finally, the data shows (Fig. 6(e),(f)) that our participants saw the dots to be within a *size* range, for both paper and screen conditions. Particularly interesting are the results for 0.50 dots: here results differ depending on the paper type, whereas the paper type did not seem to matter much for 0.20 and 0.13 dots. Nonetheless, in all cases people perceived the dots to be different in size, consistent between paper and screen display (Fig. 8(e)).

Clustered five-tone tests. Here our data shows that our participants were able to accurately and precisely perceive the *tone* of the ramps for the display condition (Fig. 7(a)), while in the paper condition they perceived much darker tones (almost black) than intended (Fig. 7(b)). This observation is consistent for all paper types and tip sizes, and is also consistent in the difference between paper and display conditions (Fig. 8(b)). This result could explain why many people consider stippling as black-and-white-only technique. Our result also implies that the print reproduction of stippling via documents such as PDF will usually produce results different from what was initially intended.

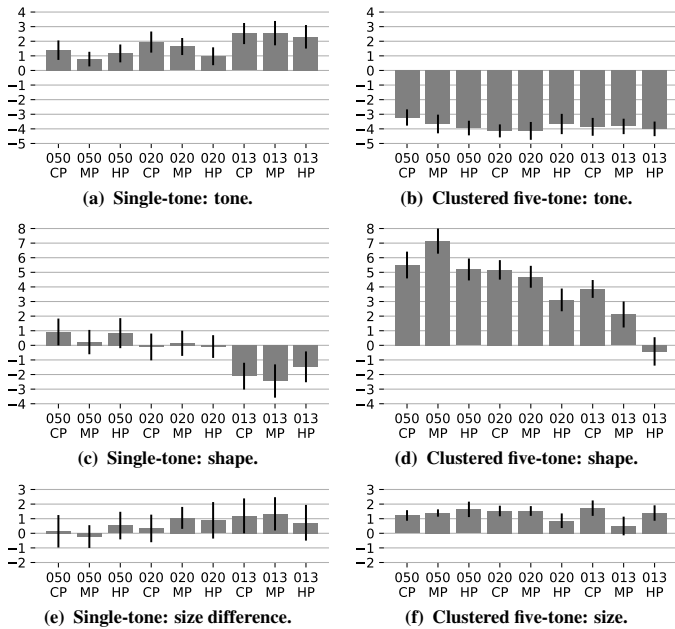


Fig. 8. Means of the pairwise differences between display and paper conditions (paper – display); error bars: 95% CIs.

The fact that the *shape* of the dots is not round was detected for the display condition (Fig. 7(c)), yet overall our participants perceived the dots to be more circular than they actually were. In contrast, in the paper condition the participants perceived the dots to be much more irregular than they really were (Fig. 8(d); except for the 0.13 dots on hot-press paper), and generally more irregular than they actually were (Fig. 7(d), except for the small 0.13 dots). These differences should be investigated further, but may be related to the small pixel size for the screen reproduction, the halftoning used for the print reproduction, and probably the “dot gain” effect we mentioned in Sect. 4.1.

The dots’ *size*, finally, was perceived accurately but less precisely for both the paper and screen conditions (Fig. 7(e),(f)), with participants thinking that the size was a bit larger than their actual size. This difference is consistently more pronounced for printer reproduction than for viewing on displays (Fig. 8(f)), yet is rather small overall.

Discussion of hypotheses. We did not confirm **H1** in general as no dots in the isolated single-tone test were seen as black. Quite in contrast to what we thought, in particular small dots were seen as having a gray color. **H1(a)**, however, is fully confirmed for realistic mixes of point densities: all dots in the clustered tests are perceived as almost black when printed. It is important to also note the regularity of the results.

Next, we did not confirm **H2**: all dots were seen as irregular (so only confirming **H2(a)**, and **H2(b)** for 0.50 dots, but probably not our reasoning about them), yet with paper type not making a big difference. Next, we also could not generally confirm **H3**—the size differences between the dots were generally perceived for all paper types and tip sizes, maybe with the only exception of 0.50 dots on hot-press paper for which participants saw the least size difference.

All these hypotheses applied to the isolated single-tone tests. When considered for the clustered five-tone tests, however, a

different picture emerges. For example, **H1** for paper could be seen as confirmed, yet for all dot sizes and not only for the small ones. Similarly, a trend as described in **H2** seems to emerge for the print condition, with smaller dots seen as more rounded than larger ones. For the display condition all dots seemed to be perceived as more rounded than their actual shape. Finally, we confirmed **H4**, yet with a variation different from what we expected: our participants accurately perceived dot tones and sizes for both print and screen reproduction, their responses being more precise for displays than for printers. They had more issues, however, with matching dot shapes to the correct sample.

5.2.7. Limitations

While we have used a careful and data-driven design, implementation, and realization of our study, it still has some limitations. Here we discuss the most important ones.

First, we used simplified stimuli as it is common in perceptual studies [76, Sec. 3.5]: stippled fields of a single-tone or ramps of several tones. We made this choice because we wanted to test the influence of the stipple dots independent from other confounding factors such as the content of a stippled image. So while we did not use realistic stippled images, our results generalize to those the same way that gray ramps and Fourier-transformed frequency analyses are used in studying stipple dot distributions.

Another limitation is that our set of scanned dots comes from a single artist. While drawing a dot with a pen is straightforward, it is possible that other artists would produce different dots. Second, in our study we were limited by the amount of time a participant spend, limiting the number of possible comparisons. In addition, we had to choose a particular group of participants, in our case fine arts students. This choice, naturally, had implications on the female/male proportion as well as the age distribution of our participant pool.

In our study design we did our best to avoid order effects, in our case using a Latin-squares design. Nonetheless, we could not achieve all different combinations that way due to the limited number of participants we could reasonably test. So we had to resort to randomization of those aspects which we thought were least likely to cause order effects. Next, our design relied on specific distance from the viewer to the paper or screen, computed based on our previous considerations. While we continuously reminded our participants to maintain this distance, it was not physically enforced. Consequently a small error may have been introduced. Also, we printed on common 80 g/m² recycled white paper. While better-quality papers exist as well, this would have dramatically increased the material cost since every participant received a uniquely ordered stack of printed samples. While most current displays can only reproduce sRGB colors in the best case, limiting the available color and also grayscale gamut and a better display than the one we used may have produced better results. Finally, the results in our pilot study may have been affected by the fact that we asked participants to focus specifically on the three dot characteristics, yet other and more indirect forms of studying the perception of the effects would have likely been subject to even higher subjective errors. Overall, however, we do not believe that any of these effects endangers the validity of our results.

6. Implications of our Results

The conclusions from both our detailed discussion of scanned samples of stipple dots (Sections 3 and 4) as well as of our perceptual studies on how people perceive hand-made stipple dots (Sect. 5) are the following:

1. Real stipple dots are not black circles but they have different tones, shapes, and size ranges, which depend on the tip size of the used pen and the used paper type.
2. The differences of these attributes can be perceived by people when they look at original stipple artwork.
3. Faithfully represented dots are perceived differently depending on whether they are shown on a display or the use of print reproduction, so the replication of these attributes depends on the output medium and should be targeted specifically to the intended medium.

The first finding is not necessarily new [41, 42] or surprising, it results from the interaction of the ink from the pen with the paper onto which the pen deposits the ink. With this article we demonstrated the specific interactions of pen size and paper type as well as the resulting characteristics of the produced dots, and that people do perceive that real dots are not necessarily all circular, without texture, and all of the same size—our second main finding. However, we also wanted to understand if these characteristics would be perceived by people looking at computer-made stippled images (within the constraints of a controlled experiment—in our case stippling of simple gray ramps), depending on the reproduction medium. Our results and, in particular, those of the clustered five-tone tests (which are most representative of practical application cases) clearly show—which is our third finding—that people do perceived the dot characteristics, yet differently depending on whether the images are shown on a computer display or printed on paper.

On regular displays, our participants were able to match the real tones and sizes with great accuracy, with a small bias toward larger than normal sizes—consistent for all paper and pen tip combinations. In contrast, displays were not able to reproduce dot shapes correctly, generally making the dots appear rounder than normal. When looking at samples printed on paper, our participants were also able to match the real tones and sizes with accuracy, but with less precision, showing a large bias toward black in the case of tone, and a bias toward larger dots in the case of size. Laser printing consistently leads to a perception of a darker tone because its inherent limitation to reproduce tone shades—it is thus largely a black-and-white medium and even the use of halftoning to replicate correct tonal textures does not improve the result. This may explain why stippling has traditionally been considered as a B&W-only technique, but it is important to note that this notion cannot be extended to displays. The reproduction of shape, finally, is better for printing than for displays, but not very consistently. We note that these aspects of stipple dot perception in printing imply that, for small dots, stipple dot textures and sizes matter less and stippling becomes a technique quite similar to halftoning.

We also saw that pixel resolution plays an important rule for a faithful replication of stippling. Because current common

display hardware⁵ does not have the sufficient resolution to display faithfully created stipple images, it also does not yet make sense to use displays as the primary output medium, but this is likely to change in the future.

Yet even today's limited displays need to be used as a tool for the production of digital stippling by artists and illustrators. The respective tools thus not only have to work at a much higher resolution than is shown on the display, but the tool also has to show both a correctly scaled representation of the produced work as well as zoomed-in versions to see the detail. Only with such a focus+context view will it be possible for the artists to work at both overview and detail levels—as they are used to in their traditional practice. Moreover, the tools have to provide means to output the result in several different versions: a high-resolution grayscale (color) version, a high-resolution 1 bit version that only captures the stipple shapes, and potentially a version that uses the 1 stipple = 1 pixel convention. A vector graphic output (as it is sometimes advocated for NPR work [77]) would be useful if it captures the shape of the stipples at a high pixel density, which would avoid the re-sampling of 1 bit raster images at the printer. In the future, maybe there will be vector graphic languages that also are capable to capture the texture faithfully—some initial attempts in this direction have already been presented [78–83].

The implications for print reproduction arise from certain assumed standards in the publishing domain. In particular, publishers frequently ask for 300 ppi images for material intended to be printed (in academic publishing and elsewhere). As we have seen, this pixel density is neither sufficient to reproduce stippling in full fidelity, nor does it suffice for a shape-only black-and-white reproduction. In these cases one has to try to convince the publishers of the specific needs of stippling as a medium, and at least aim for 1200 ppi in 1 bit black-and-white mode to be able to capture the stipple shapes—a representation that uses similar or less bandwidth than a 300 ppi grayscale or full color image [77]. If publishers do not impose a limit such as 300 ppi for images, of course, one can and should embed results with higher pixel densities since imagesetter hardware supports ≥ 2400 dpi. Yet even with such high-quality output we need to take the results of our experiment into account which indicate that a correct tone perception of the reproduced images is difficult, which means that one may be limited to a faithful reproduction of shape and size and represent the dots in black-and-white.

These implications for print reproduction and display on a screen also affect those media forms that were created for both forms of output, such as PDF or Postscript documents. Here we face the diverging capabilities/constraints that cannot be met at the same time. A good compromise seems to be, as just mentioned, to use 1 bit black-and-white images—it both prints well and can also be used to display good versions on a screen through interpolation, at the intended or at a zoomed-in scale, albeit at the expense of loosing the stipple textures (tone). Future media may provide different versions of the embedded images (i. e., stipple dot textures) based on the present output device

⁵Recent high-end laptops with UHD displays almost reach a of 300 ppi, while state-of-the-art PCs such as Microsoft's Surface Studio and Apple's iMac 5k 27" still only reach 192 ppi and 217 ppi, respectively. Dell's 32" 8K UltraSharp UP3218K. reaches the 280 ppi.

and the currently employed zoom. One way to use and even improve on this concept would be to replace scanned dots with synthesized stipple dot textures.

Overall, displays and printers thus produce different results. In the case of a general use, displays are better because they accurately represent two of the three characteristics of dots. For a concrete characteristic, however, our study and discussion allow practitioners to select the best suited device for an application (e. g., to use displays if a faithful reproduction of tone is required, or if shape is to be reproduced well then a high-resolution print reproduction is better).

7. Conclusion

The evolution of techniques and computing hardware allows us to (re-)produce stippling at an ever-increasingly quality. While researchers concentrated mostly on stipple point distributions versus the dot attributes in the past, we showed that it is also important to consider the reproduction of the dots themselves, specifically, for the realistic production of hand-made stippling, but also, for those results that want to consider the perception as an important component.

Our work thus specifically provides a better insight on the size, shape, and texture of real stipple dots. Our discussion of the observed was mostly driven by the ultimate goal of producing tools to be used by artists and illustrators—a goal that has been one of the driving forces of much of the work in NPR. We are convinced that we have made progress toward this goal with our discussion and the insights that we present in this paper.

In the future it may be worth considering the implications the decisions that are made at the instrumental task level. For example, the use of pens with small nib sizes and hot press papers not only increases the possible stipple dot numbers/frequencies but also leads to a darker tone, more similar sizes, and more regular shapes. Such characteristics better suit the existing forms of reproduction and produce stipple dots like used in NPR in the past, albeit these are still not perfect circles in pure black.

As we also discussed in Sect. 3, both our work and much of the past work in NPR stippling only addresses the instrumental task of stippling and leaves the artistic and procedural tasks largely untouched. The (at least partial) support of these activities in NPR tools, we believe however, are necessary to create tools that will have a practical impact for artists and illustrators and should thus become a much more important aspect of future NPR work.

Finally, it may also be interesting to consider dedicated output devices that physically reproduce some of the low-level aspects of the instrumental task. Plotters, for example, could be equipped with a physical pen and used for realistic output of stipple images, similar to what others have explored with robots for NPR-based oil painting [84–86], portrait drawing [87], or Chinese painting [88]. The use of such a setup may even allow us to better control perceptual studies like the ones we described in this paper as it promises to remove much of the human-cause variability in the placement of individual dots, and we could fully control and replicate the used dot distributions.

Acknowledgments

We thank Miguel Endara, Randy Glass, and Elena Piñar for the permission to use their artwork in our paper. We also thank Ana Belén Cruz for the samples we used in our discussion and Lonni Besançon for help with the statistical analysis of our data. This work has partially been funded by the Ministry of Economy, Industry and Competitiveness of Spain through the project TIN 2017-85259-R with FEDER funds.

References

- [1] Strothotte, T, Schlechtweg, S. Non-Photorealistic Computer Graphics. Modeling, Animation, and Rendering. San Francisco: Morgan Kaufmann; 2002. doi:10.1016/B978-1-55860-787-3.50019-0.
- [2] Deussen, O, Isenberg, T. Halftoning and stippling. In: Rosin, P, Collomosse, J, editors. Image and Video based Artistic Stylisation; vol. 42 of *Computational Imaging and Vision*; chap. 3. London/Heidelberg: Springer; 2013, p. 45–61. doi:10.1007/978-1-4471-4519-6_3.
- [3] Kyprianidis, JE, Collomosse, J, Wang, T, Isenberg, T. State of the “art”: A taxonomy of artistic stylization techniques for images and video. *IEEE Transactions on Visualization and Computer Graphics* 2013;19(5):866–885. doi:10.1109/TVCG.2012.160.
- [4] Martín, D, Arroyo, G, Rodríguez, A, Isenberg, T. A survey of digital stippling. *Computers & Graphics* 2017;67:24–44. doi:10.1016/j.cag.2017.05.001.
- [5] Meruvia Pastor, OE, Freudenberg, B, Strothotte, T. Real-time animated stippling. *IEEE Computer Graphics and Applications* 2003;23(4):62–68. doi:10.1109/MCG.2003.1210866.
- [6] Martín, D, del Sol, V, Romo, C, Isenberg, T. Drawing characteristics for reproducing traditional hand-made stippling. In: Proc. NPAR. Goslar, Germany: Eurographics Assoc.; 2015, p. 103–115. doi:10.2312/exp.20151183.
- [7] Lloyd, SP. Least squares quantization in PCM. *IEEE Transactions on Information Theory* 1982;28(2):129–137. doi:10.1109/TIT.1982.1056489.
- [8] McCool, M, Fiume, E. Hierarchical Poisson disk sampling distributions. In: Proc. Graphics Interface. San Francisco: Morgan Kaufmann Publishers Inc.; 1992, p. 94–105. doi:10.20380/GI1992.12.
- [9] Deussen, O, Hiller, S, van Overveld, C, Strothotte, T. Computer-generated stipple drawings. In: Proc. VMV. Sankt Augustin, Germany: infix; 1999, p. 329–338.
- [10] Deussen, O, Hiller, S, van Overveld, C, Strothotte, T. Floating points: A method for computing stipple drawings. *Computer Graphics Forum* 2000;19(3):41–50. doi:10.1111/1467-8659.00396.
- [11] Secord, A. Weighted Voronoi stippling. In: Proc. NPAR. New York: ACM; 2002, p. 37–43. doi:10.1145/508530.508537.
- [12] Hiller, S, Hellwig, H, Deussen, O. Beyond stippling – Methods for distributing objects on the plane. *Computer Graphics Forum* 2003;22(3):515–522. doi:10.1111/1467-8659.00699.
- [13] Dalal, K, Klein, AW, Liu, Y, Smith, K. A spectral approach to NPR packing. In: Proc. NPAR. New York: ACM; 2006, p. 71–78. doi:10.1145/1124728.1124741.
- [14] Secord, A, Heidrich, W, Streit, L. Fast primitive distribution for illustration. In: Proc. EGWR. Goslar, Germany: Eurographics Assoc.; 2002, p. 215–226. doi:10.2312/EGWR/EGWR02/215-226.
- [15] Arroyo, G, Martín, D, Luzón, MV. Stochastic generation of dots for computer aided stippling. *Computer-Aided Design and Applications* 2010;7(4):447–463. doi:10.3722/cadaps.2010.447-463.
- [16] Schlechtweg, S, Germer, T, Strothotte, T. Renderbots—Multi-agent systems for direct image generation. *Computer Graphics Forum* 2005;24(2):137–148. doi:10.1111/j.1467-8659.2005.00838.x.
- [17] Hodges, ERS, editor. *The Guild Handbook of Scientific Illustration*. 2nd ed.; Hoboken, NJ, USA: John Wiley & Sons; 2003. URL: <http://www.wiley.com/remtitle.cgi?isbn=0471360112>.
- [18] Balzer, M, Schlömer, T, Deussen, O. Capacity-constrained point distributions: A variant of Lloyd’s method. *ACM Transactions on Graphics* 2009;28(3):86:1–86:8. doi:10.1145/1531326.1531392.

- [19] Kopf, J, Cohen-Or, D, Deussen, O, Lischinski, D. Recursive Wang tiles for real-time blue noise. *ACM Transactions on Graphics* 2006;25(3):509–518. doi:[10.1145/1141911.1141916](https://doi.org/10.1145/1141911.1141916).
- [20] Ascencio-Lopez, I, Meruvia-Pastor, O, Hidalgo-Silva, H. Adaptive incremental stippling using the Poisson-disk distribution. *Journal of Graphics, GPU, and Game Tools* 2010;15(1):29–47. doi:[10.1080/2151237X.2010.10390650](https://doi.org/10.1080/2151237X.2010.10390650).
- [21] Deussen, O, Spicker, M, Zheng, Q. Weighted linde-buzo-gray stippling. *ACM Transactions on Graphics* 2017;36(6):233:1–233:12. doi:[10.1145/3130800.3130819](https://doi.org/10.1145/3130800.3130819).
- [22] Deussen, O. Aesthetic placement of points using generalized Lloyd relaxation. In: *Proc. CAE. Goslar, Germany: Eurographics Assoc.; 2009*, p. 123–128. doi:[10.2312/COMPAESTH/COMPAESTH09/123-128](https://doi.org/10.2312/COMPAESTH/COMPAESTH09/123-128).
- [23] Meruvia Pastor, OE, Strothotte, T. Frame-coherent stippling. In: *Eurographics Short Presentations. Goslar, Germany: Eurographics Assoc.; 2002*, p. 145–152. doi:[10.2312/egs.20021002](https://doi.org/10.2312/egs.20021002).
- [24] Lu, A, Taylor, J, Hartner, M, Ebert, DS, Hansen, CD. Hardware-accelerated interactive illustrative stipple drawing of polygonal objects. In: *Proc. VMV. Aka GmbH; 2002*, p. 61–68. URL: http://www.ecn.purdue.edu/purpl/level2/papers/stipple_VMV_2002.pdf.
- [25] Lu, A, Morris, CJ, Taylor, J, Ebert, DS, Hansen, C, Rheingans, P, et al. Illustrative interactive stipple rendering. *IEEE Transactions on Visualization and Computer Graphics* 2003;9(2):127–138. doi:[10.1109/TVCG.2003.1196001](https://doi.org/10.1109/TVCG.2003.1196001).
- [26] Meruvia Pastor, OE, Strothotte, T. Graph-based point relaxation for 3D stippling. In: *Proc. Mexican International Conference on Computer Science. Los Alamitos: IEEE Computer Society; 2004*, p. 145–152. doi:[10.1109/ENC.2004.1342599](https://doi.org/10.1109/ENC.2004.1342599).
- [27] Yuan, X, Nguyen, MX, Zhang, N, Chen, B. Stippling and silhouettes rendering in geometry-image space. In: *Proc. EGSR. Goslar, Germany: Eurographics Assoc.; 2005*, p. 193–200. doi:[10.2312/EGWR/EGSR05/193-200](https://doi.org/10.2312/EGWR/EGSR05/193-200).
- [28] Vanderhaeghe, D, Barla, P, Thollot, J, Sillion, FX. Dynamic point distribution for stroke-based rendering. In: *Rendering Techniques. Goslar, Germany: Eurographics Assoc.; 2007*, p. 139–146. doi:[10.2312/EGWR/EGSR07/139-146](https://doi.org/10.2312/EGWR/EGSR07/139-146).
- [29] Xu, H, Chen, B. Stylized rendering of 3D scanned real world environments. In: *Proc. NPAR. New York: ACM; 2004*, p. 25–34. doi:[10.1145/987657.987662](https://doi.org/10.1145/987657.987662).
- [30] Zakaria, N, Seidel, HP. Interactive stylized silhouette for point-sampled geometry. In: *Proc. GRAPHITE. New York: ACM; 2004*, p. 242–249. doi:[10.1145/988834.988876](https://doi.org/10.1145/988834.988876).
- [31] Foster, K, Jepp, P, Wyvill, B, Costa Sousa, M, Galbraith, C, Jorge, JA. Pen-and-ink for BlobTree implicit models. *Computer Graphics Forum* 2005;24(3):267–276. doi:[10.1111/j.1467-8659.2005.00851.x](https://doi.org/10.1111/j.1467-8659.2005.00851.x).
- [32] Schmidt, R, Isenberg, T, Jepp, P, Singh, K, Wyvill, B. Sketching, scaffolding, and inking: A visual history for interactive 3D modeling. In: *Proc. NPAR. New York: ACM; 2007*, p. 23–32. doi:[10.1145/1274871.1274875](https://doi.org/10.1145/1274871.1274875).
- [33] Pfister, H, Zwicker, M, van Baar, J, Gross, M. Surfels: Surface elements as rendering primitives. In: *Proc. SIGGRAPH. New York: ACM. ISBN 1-58113-208-5; 2000*, p. 335–342. doi:[10.1145/344779.344936](https://doi.org/10.1145/344779.344936).
- [34] Vital Brazil, E, Macêdo, I, Costa Sousa, M, Velho, L, de Figueiredo, LH. A few good samples: Shape & tone depiction for Hermite RBF implicits. In: *Proc. NPAR. New York: ACM; 2010*, p. 7–15. doi:[10.1145/1809939.1809941](https://doi.org/10.1145/1809939.1809941).
- [35] Lu, A, Morris, CJ, Ebert, DS, Rheingans, P, Hansen, C. Non-photorealistic volume rendering using stippling techniques. In: *Proc. VIS. Los Alamitos: IEEE Computer Society; 2002*, p. 211–218. doi:[10.1109/VISUAL.2002.1183777](https://doi.org/10.1109/VISUAL.2002.1183777).
- [36] Barla, P, Breslav, S, Markosian, L, Thollot, J. Interactive hatching and stippling by example. *Tech. Rep.; INRIA; 2006*. URL: <http://artis.imag.fr/Publications/2006/BBMT06>.
- [37] Barla, P, Breslav, S, Thollot, J, Sillion, FX, Markosian, L. Stroke pattern analysis and synthesis. *Computer Graphics Forum* 2006;25(3):663–671. doi:[10.1111/j.1467-8659.2006.00986.x](https://doi.org/10.1111/j.1467-8659.2006.00986.x).
- [38] Maciejewski, R, Isenberg, T, Andrews, WM, Ebert, DS, Sousa, MC. Aesthetics of hand-drawn vs. computer-generated stippling. In: *Proc. CAE. Goslar, Germany: Eurographics Assoc.; 2007*, p. 53–56. doi:[10.2312/COMPAESTH/COMPAESTH07/053-056](https://doi.org/10.2312/COMPAESTH/COMPAESTH07/053-056).
- [39] Maciejewski, R, Isenberg, T, Andrews, WM, Ebert, DS, Costa Sousa, M, Chen, W. Measuring stipple aesthetics in hand-drawn and computer-generated images. *IEEE Computer Graphics and Applications* 2008;28(2):62–74. doi:[10.1109/MCG.2008.35](https://doi.org/10.1109/MCG.2008.35).
- [40] Kim, S, Maciejewski, R, Isenberg, T, Andrews, WM, Chen, W, Costa Sousa, M, et al. Stippling by example. In: *Proc. NPAR. New York: ACM; 2009*, p. 41–50. doi:[10.1145/1572614.1572622](https://doi.org/10.1145/1572614.1572622).
- [41] Martín, D, Arroyo, G, Luzón, MV, Isenberg, T. Example-based stippling using a scale-dependent grayscale process. In: *Proc. NPAR. New York: ACM; 2010*, p. 51–61. doi:[10.1145/1809939.1809946](https://doi.org/10.1145/1809939.1809946).
- [42] Martín, D, Arroyo, G, Luzón, MV, Isenberg, T. Scale-dependent and example-based stippling. *Computers & Graphics* 2011;35(1):160–174. doi:[10.1145/1809939.1809946](https://doi.org/10.1145/1809939.1809946).
- [43] Hausner, A. Pointillist halftoning. In: *Proc. CGIM. Calgary, AB, Canada: ACTA Press; 2005*, p. 134–139. URL: <http://www.actapress.com/Abstract.aspx?paperId=21369>.
- [44] Mould, D. Stipple placement using distance in a weighted graph. In: *Proc. CAE. Goslar, Germany: Eurographics Assoc.; 2007*, p. 45–52. doi:[10.2312/COMPAESTH/COMPAESTH07/045-052](https://doi.org/10.2312/COMPAESTH/COMPAESTH07/045-052).
- [45] Li, H, Mould, D. Structure-preserving stippling by priority-based error diffusion. In: *Proc. Graphics Interface. Waterloo, ON, Canada: CHCCS; 2011*, p. 127–134. doi:[10.20380/GI2011.17](https://doi.org/10.20380/GI2011.17).
- [46] Kim, D, Son, M, Lee, Y, Kang, H, Lee, S. Feature-guided image stippling. *Computer Graphics Forum* 2008;27(4):1209–1216. doi:[10.1111/j.1467-8659.2008.01259.x](https://doi.org/10.1111/j.1467-8659.2008.01259.x).
- [47] Kim, S, Woo, I, Maciejewski, R, Ebert, D. Automated hedcut illustration using isophotes. In: *Proc. Smart Graphics. Berlin/Heidelberg: Springer; 2010*, p. 172–183. doi:[10.1007/978-3-642-13544-6_17](https://doi.org/10.1007/978-3-642-13544-6_17).
- [48] Son, M, Lee, Y, Kang, H, Lee, S. Structure grid for directional stippling. *Graphical Models* 2011;73(3):74–87. doi:[10.1016/j.gmod.2010.12.001](https://doi.org/10.1016/j.gmod.2010.12.001).
- [49] Gatys, LA, Ecker, AS, Bethge, M. A neural algorithm of artistic style. *arXiv.org report 1508.06576; 2015*. URL: <https://arxiv.org/abs/1508.06576>.
- [50] Gatys, LA, Ecker, AS, Bethge, M. Image style transfer using convolutional neural networks. In: *Proc. CVPR. Los Alamitos: IEEE Computer Society; 2016*, p. 2414–2423. doi:[10.1109/CVPR.2016.265](https://doi.org/10.1109/CVPR.2016.265).
- [51] Semmo, A, Isenberg, T, Döllner, J. Neural style transfer: A paradigm shift for image-based artistic rendering? In: *Proc. NPAR. New York: ACM; 2017*, p. 5:1–5:13. doi:[10.1145/3092919.3092920](https://doi.org/10.1145/3092919.3092920).
- [52] Marr, D. *Vision*. The MIT Press; 1982. ISBN 978-0-262-51462-0.
- [53] Sousa, MC, Buchanan, JW. Computer-generated graphite pencil rendering of 3D polygonal models. *Computer Graphics Forum* 1999;18(3):195–207. doi:[10.1111/1467-8659.00340](https://doi.org/10.1111/1467-8659.00340).
- [54] Sousa, MC, Buchanan, JW. Observational model of graphite pencil materials. *Computer Graphics Forum* 2000;19(1):27–49. doi:[10.1111/1467-8659.00386](https://doi.org/10.1111/1467-8659.00386).
- [55] AlMeraj, Z, Wyvill, B, Isenberg, T, Gooch, AA, Guy, R. Automatically mimicking unique hand-drawn pencil lines. *Computers & Graphics* 2009;33(4):496–508. doi:[10.1016/j.cag.2009.04.004](https://doi.org/10.1016/j.cag.2009.04.004).
- [56] Curtis, CJ, Anderson, SE, Seims, JG, Fleischer, KW, Salesin, DH. Computer-generated watercolor. In: *Proc. SIGGRAPH. New York: ACM; 1997*, p. 421–430. doi:[10.1145/258734.258896](https://doi.org/10.1145/258734.258896).
- [57] Chu, N, Baxter, W, Wei, LY, Govindaraju, N. Detail-preserving paint modeling for 3D brushes. In: *Proc. NPAR. New York: ACM; 2010*, p. 27–34. doi:[10.1145/1809939.1809943](https://doi.org/10.1145/1809939.1809943).
- [58] Lu, J, Barnes, C, DiVerdi, S, Finkelstein, A. Realbrush: Painting with examples of physical media. *ACM Transactions on Graphics* 2013;32(4):117:1–117:12. doi:[10.1145/2461912.2461998](https://doi.org/10.1145/2461912.2461998).
- [59] Rudolf, D, Mould, D, Neufeld, E. A bidirectional deposition model of wax crayons. *Computer Graphics Forum* 2005;24(1):27–39. doi:[10.1111/j.1467-8659.2005.00826.x](https://doi.org/10.1111/j.1467-8659.2005.00826.x).
- [60] DiVerdi, S, Krishnaswamy, A, Mëch, R, Ito, D. Painting with polygons: A procedural watercolor engine. *IEEE Transactions on Visualization and Computer Graphics* 2013;19(5):723–735. doi:[10.1109/TVCG.2012.295](https://doi.org/10.1109/TVCG.2012.295).
- [61] Ulichney, R. *Digital Halftoning*. MIT Press; 1987. ISBN 978-0-262-21009-6. URL: <https://mitpress.mit.edu/books/digital-halftoning>.
- [62] Blatner, D, Roth, S. *Real World Scanning and Halftones*. Peachpit Press; 1993. URL: <http://www.peachpit.com/store/real-world-scanning-and-halftones-9780321241320>.
- [63] Green, P. *Understanding Digital Color*. 2nd ed.; GATF Press; 1999.
- [64] Pollaris, M, Tas, J, Vandezande, M, editors. *An Introduction to Digital*

- Scanning; vol. 4 of *Digital Color Prepress*. Morsel, Belgium: Agfa-Gevaert N.V.; 1994. URL: <https://www.scribd.com/document/47211346/An-Introduction-to-Digital-Scanning>.
- [65] ICO Visual Functions Committee. Visual acuity measurement standard. Standard; International Council of Ophthalmology; 1984. URL: <http://www.icoph.org/dynamic/attachments/resources/icovisualacuity1984.pdf>.
- [66] Lau, DL, Arce, GR, Gallagher, NC. Digital halftoning by means of green-noise masks. *Journal of the Optical Society of America* 1999;16(7):1575–1586. doi:10.1364/JOSAA.16.001575.
- [67] Floyd, RW, Steinberg, L. An adaptative algorithm for spatial gray scale. *Proceedings of the Society of Information Display* 1976;(7):75–77.
- [68] Ostromoukhov, V. A simple and efficient error-diffusion algorithm. In: *Proc. SIGGRAPH*. New York: ACM; 2001, p. 567–572. doi:10.1145/383259.383326.
- [69] Likert, RA. A technique for the measurement of attitudes. *Archives of Psychology* 1932;22(140):5–55.
- [70] Efron, B. Bootstrap methods: Another look at the jackknife. *The Annals of Statistics* 1979;7(1):1–26. doi:10.1214/aos/1176344552.
- [71] VandenBos, GR, editor. *Publication Manual of the American Psychological Association*. 6th ed.; Washington, DC: APA; 2009. URL: <http://www.apastyle.org/manual/>.
- [72] Baker, M. Statisticians issue warning over misuse of P values. *Nature News* 2016;531(7593):151. doi:10.1038/nature.2016.19503.
- [73] Cumming, G. The new statistics. *Psychological Science* 2013;25(1):7–29. doi:10.1177/0956797613504966.
- [74] Dragicevic, P. Fair statistical communication in HCI. In: Robertson, J, Kaptein, M, editors. *Modern Statistical Methods for HCI*; chap. 13. Cham, Switzerland: Springer International Publishing; 2016, p. 291–330. doi:10.1007/978-3-319-26633-6_13.
- [75] Krzywinski, M, Altman, N. Points of significance: Error bars. *Nature Methods* 2013;10(10):921–922. doi:10.1038/nmeth.2659.
- [76] Kosara, R, Haroz, S. Skipping the replication crisis in visualization: Threats to study validity and how to address them. In: *Proc. BELIV*. Los Alamitos: IEEE Computer Society; 2018, p. 102–107. doi:10.1109/BELIV.2018.8634392.
- [77] Isenberg, T, Carpendale, MST, Sousa, MC. Breaking the pixel barrier. In: *Proc. CAE*. Goslar, Germany: Eurographics Assoc.; 2005, p. 41–48. doi:10.2312/COMPAESTH/COMPAESTH05/041-048.
- [78] Sun, J, Liang, L, Wen, F, Shum, HY. Image vectorization using optimized gradient meshes. *ACM Transactions on Graphics* 2007;26:11:1–11:7. doi:10.1145/1276377.1276391.
- [79] Orzan, A, Bousseau, A, Winnemöller, H, Barla, P, Thollot, J, Salesin, D. Diffusion Curves: A vector representation for smooth-shaded images. *ACM Transactions on Graphics* 2008;27(3):92:1–92:8. doi:10.1145/1360612.1360691.
- [80] Bezerra, H, Eisemann, E, DeCarlo, D, Thollot, J. Diffusion constraints for vector graphics. In: *Proc. NPAR*. New York: ACM; 2010, p. 35–42. doi:10.1145/1809939.1809944.
- [81] Jeschke, S, Cline, D, Wonka, P. Estimating color and texture parameters for vector graphics. *Computer Graphics Forum* 2011;30(2):523–532. doi:10.1111/j.1467-8659.2011.01877.x.
- [82] Barla, P, Bousseau, A. Gradient art: Creation and vectorization. In: Rosin, P, Collomosse, J, editors. *Image and Video based Artistic Stylisation*; vol. 42 of *Computational Imaging and Vision*; chap. 8. London, Heidelberg: Springer; 2013, p. 149–166. doi:10.1007/978-1-4471-4519-6_8.
- [83] Benjamin, MD, DiVerdi, S, Finkelstein, A. Painting with triangles. In: *Proc. NPAR*. New York: ACM; 2014, p. 13–20. doi:10.1145/2630397.2630399.
- [84] Haggerty, M. Robotic painting: Art creating art. *IEEE Computer Graphics and Applications* 1992;12(4):8–10. doi:10.1109/MCG.1992.10027.
- [85] Deussen, O, Lindemeier, T, Pirk, S, Tautzenberger, M. Feedback-guided stroke placement for a painting machine. In: *Proc. CAE*. Goslar, Germany: Eurographics Assoc.; 2012, p. 63–70. doi:10.2312/COMPAESTH/COMPAESTH12/025-033.
- [86] Lindemeier, T, Metzner, J, Pollak, L, Deussen, O. Hardware-based non-photorealistic rendering using a painting robot. *Computer Graphics Forum* 2015;34(2):311–323. doi:10.1111/cgf.12562.
- [87] Tresset, P, Leymarie, FF. Portrait drawing by Paul the robot. *Computers & Graphics* 2013;37(5):348–363. doi:10.1016/j.cag.2013.01.012.
- [88] Yao, F, Shao, G. Painting brush control techniques in Chinese painting robot. In: *Proc. ROMAN*. Los Alamitos: IEEE Computer Society; 2005,

p. 462–467. doi:10.1109/ROMAN.2005.1513822.

Appendix A. Stipple Dot Synthesis

For our study we needed an interpolation between the original scanned dots and circular dots, as well as an extrapolation of the original scanned dots to produce more irregular shapes. For the interpolation process, we considered to use simple methods as linear interpolation between two different dots, but this produces ghosting artifacts, specially for bigger dots. For the extrapolation, there is no easy methods either. For all these cases, we have developed new methods based on energy diffusion.

Our main assumption for this approach is that scans can best capture the properties of real ink diffusion in paper. We thus developed two techniques that work with different inputs and different goals. The first version interpolates between a circle and a real dot using a physically inspired ink expansion process from the dot’s center to the outside. The second approach produces extrapolated and thus, more exaggerated versions of a real dot. These algorithms yield a list of sorted images with each step of the interpolation as shown in Fig. A.9.

Appendix A.1. From a circle to a scanned stipple dot

The goal of this first approach is to provide a transition from circular stipple dot (as historically used in digital stippling) into a given scan of a real dot. For this purpose we consider the ink of the stipples as a form of energy, so a circular dot could be seen as a configuration of equilibrium of a dot’s energy. Our approach thus iteratively moves the ink from the center toward the real dot to transition from the circle to a real scan. We thus first formulate the complete energy of a given target dot as

$$E(S) = \int_A e(x) dx \quad (\text{A.1})$$

where S represents the real scan, E is the function of energy, A is the area containing the dot, and e is the function that returns the energy for some given area. We discretize the space by subdividing it using a regular grid into cells (i. e., pixels of the dot’s scan). We then approximate the center of a given dot scan (S) as its centroid (C):

$$C(S) = \frac{1}{E(S)} \sum_i e(x_i) \cdot x_i \quad (\text{A.2})$$

where e computes the energy in some discrete area and x_i represents every cell with some amount of energy, also treating $E(S)$ from Eq. A.1 in its discretized form.

To define a circular stipple equivalent to the scanned dot we then determine the effective radius of the scanned dot ($R(S)$) based on its total energy ($E(S)$), assuming that the same energy will be equally distributed on the circle:

$$R(S) = \left\| \sqrt{E(S)/\pi} \right\| \quad (\text{A.3})$$

We iteratively move ink along the paper to interpolate from the circle that is defined by $C(S)$ and $R(S)$. Our approach behaves as a bilateral filter so, for each cell x_i of the mask of energy, the

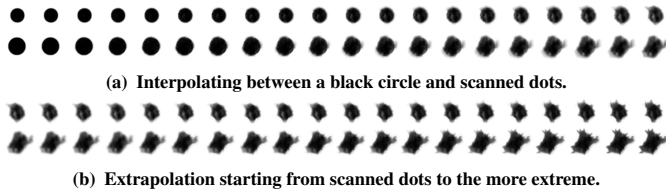


Fig. A.9. Synthesized dots as produced by the example-based algorithms.

filter function e modifies the energy of the current iteration to generate the next iteration:

$$e(x_{i+1}) = \varepsilon(x_i) \cdot [c(x_i, e(x_i)) \cdot N(x_i, I) + c^{-1}(x_i, e(x_i)) \cdot \iota(e(x_i), e_{org}(x_i)) \cdot \text{rint}(1 - \tau(1/k))] \quad (\text{A.4})$$

where control function c and its inverse c^{-1} are defined as

$$c(x, y) = \gamma(x) \cdot \tau(y) \quad (\text{A.5})$$

$$c^{-1}(x, y) = 1 - \gamma(x) \cdot \tau(y). \quad (\text{A.6})$$

Here, γ is a random function that returns either 0 or 1. It follows a linear distribution based on the distance to the center of the circle: the closer x_i is to the center, the more probable γ is to yield 1. γ thus makes cells at the perimeter of the stippling dot more reluctant to change their state, while cells closer to the center release energy more easily. Next, τ is a random function that also returns either 0 or 1. It follows an exponential distribution based on the energy at x_i : the more energy is stored in x_i , the more probable is τ to yield 1. τ thus modifies the probability of releasing energy according to a pixel's amount of energy.

The remaining terms in Eq. A.4 are as follows. ε is a mask function that returns 0 if there is no energy in the respective cell or 1 in the opposite case, thus ensuring that only cells with energy may lose energy. Next, ι is a function that returns the linear interpolation between the current state and the original dot x_i . It is affected by k that is the epoch of the current iteration. rint is the nearest integer function, passing τ to this function makes that the result becomes 0 with increasing probability as epochs pass. N , finally, is a function that swaps energy between a pixel and its eight-neighborhood, as it is described by Alg. 1.

In Alg. 1, ρ is a quantum of energy passed as parameter of the algorithm. The smaller this number is, the better the quality when transferring energy, but it also consumes more time to compute all the transitions. We have set ρ to 0.001 by default, taking into account that energy values are normalized between -1 and 1 . Negative energy values represent a transitional stage where energy is needed. At the end of the algorithm, however, no negative values remain in the mask, so the algorithm tends to fill the 'holes' of energy. Last, δ_e is the corrected accumulated error. It represents the energy that was lost due to accumulated errors when swapping energy between cells and the small amount of linear interpolated cells. It can easily be calculated by summing all the values of energy in the current state and comparing the value with the sum of the configuration of energy of the real dot.

We initialize the energy gradient ∇e by subtracting the energy of the real dot e_{org} from that of the circle e_{circle} , for each cell x_i . Negative values of ∇e are thus a request for energy, while a

Algorithm 1 Energy transfer from a cell to its neighborhood.

```

function N(x)
  for all  $x_j$  in 8-neighborhood(x) do
    if  $\nabla e(x_i) < 0$  then
       $e(x) \leftarrow e(x) - \rho$ 
       $e(x_j) \leftarrow e(x_j) + \rho + \delta_e$ 
    end if
  end for
   $e(x) \leftarrow e(x) + \delta_e$ 
end function

```

positive values represent an excess of energy. We update this gradient for each iteration after we applied filter e to all the pixels of the mask. We also implement this filter as a backtracking algorithm such that, after every iteration, we maintain both the new matrix of energy E_{new} and the previous matrix of energy E_{prev} . If E_{new} is not more similar to the energy of the real dot we repeat the process again until we get a better solution.

Note that the process described here can also easily be extended to interpolate between two actual scans of dots. For this purpose we only have to take in consideration that different dots usually have different energy. So, if we consider the ink to flow from the dot with greater energy to the dot with lesser energy, an additional step is necessary to "evaporate" the remaining energy.

Appendix A.2. Extrapolation of a scanned dot

To be able to explore people's perception of dot shapes (Sect. 5.2) we also provide a technique to extrapolate from a scanned dot toward a more extreme shape—in a way as a continuation of the circle-to-scan interpolation of Appendix A.1. While the energy of a circle moves toward the areas of energy in a scanned dot in the circle-to-scan interpolation, we now ensure that the flowing energy expands exaggerated parts and contracts concave areas.

We realize this approach in two stages. First, we compute the ink flow from the centroid of the scanned stipple dot until each one of its cells is filled with the correct amount of energy. We record these movements in a matrix of probabilities M which stores the distribution of probability for each cell of transferring ink to its eight-neighborhood.

Second, we construct a list of DESTINATIONS (Δ) which we initially populate with the scanned dot's outer contour. Δ actually contains is the cells of the grid with negative energy regarding to the previous step. This way, elements can be inserted or deleted from Δ when energy fluctuates.

Similar to the previous method, ink is flowing through the grid, altering in every step the difference of energy between the current stage of the iteration and the previous stage. This process behaves as a heat equation, balancing the energy between the stages, meaning that negative energy is a lack of ink, whereas positive energy means an excess of energy. We also store that excess of energy for each cell in a matrix named SOURCES (Σ). We dynamically update this matrix and use it as mask.

Our algorithm iterates (typically using 600–1,000 steps) in which ink propagates, while taking into account the matrix of probabilities computed in the first stage and the directions given by the contour. After this first set of iterations, we continue the ink propagation beyond the initial contour, adjusting and deforming it repeatedly (after each set of 20 steps) based on its

curvature to exaggerate its irregularities.

For each candidate at Σ , we compute the best direction to transfer ink based on M and the direction based on the best candidate at Δ . We weigh both vectors such that the final direction for a given cell is 30% the direction given by the matrix of probabilities and 70% the direction given by the contours. One can thus see M as set of probabilistic paths that mimic the natural flow of ink, whereas the contour prevents the ink from following these natural directions inexorably.

To compute M we get the centroid with Eq. A.2 and derive its corresponding Δ list and Σ mask. The matrix takes the average direction of every cell in Σ pointing to all elements in Δ (represented as dst) as the flow direction, and then we compute $M(x_{i+1})$ as

$$M(x_{i+1}) = (1 - w) \cdot M(x_i) \cdot w \cdot dst \quad (\text{A.7})$$

where we initialize M as a zero matrix and w is the learning coefficient (0.1 by default). We found that, optionally and for a more natural result, we can add a supplement coefficient in the transfer of energy to balance the energy. While the final balance of energy should return an empty mask for Σ and an empty list for Δ , accumulated precision errors could yield a list that is not empty so we need to artificially “evaporate” the excess energy for each iteration, as commented later.

Once we have determined M , we set Σ to a zero matrix and replace Δ with the contour cells of the stippling dot. Then we continue the ink transfer and modify the mask Σ . We then adjust the contours based on curvature—such that convex parts of the contour with high positive curvature get expanded, while concave parts with high negative curvature are contracted—and modify the candidates at Δ accordingly, about once every 10,000 iterations. Notice that in this case no element is removed from the list Δ because we have not defined any goal, and that with this approach the amount of energy is constantly increasing. We have thus designed a process of ‘ink evaporation’ that lowers the levels of energy of the mask when the energy passes some threshold and when the ink flows out of the boundaries defined by the extrapolated contours of the dot.

Finally, and for all the algorithms, we filter the energy that we computed in their intermediate steps using a low-pass filter and transform the resulting energy back into a grayscale image. We also analyze the difference of energy between subsequent images and select only a pre-set number of relevant images as output of the algorithms such that we receive a set of images that well represents the ink diffusion process to avoid a manual selection from a set of tens of thousands of images.

Appendix B. Additional Material

We provide the following additional material for download, along with the manuscript:

1. the dataset of the high-quality scans of stipple dot gray ramps described in Sect. 3,
2. the tool used to obtain a light tone extreme for the study described in Sect. 5.2,

3. the dataset of all data samples obtained with this tool which led to the resulting tone ramp for the study in Sect. 5.2,
4. the dataset with all synthetic gray ramps with their modifications for tone, shape, and size range used in study in Sect. 5.2, for print reproduction,
5. the program used in the study in Sect. 5.2,
6. the dataset with all anonymized participant responses in the study in Sect. 5.2 and the scripts to generate both the statistical summary and the graphs that we used for our data analysis and in the following part of the additional material,
7. additional summary statistics for the study in Sect. 5.2,
8. the program to synthesize stipple dots based on real scans described in Appendix A.